Tumor-Localized Interleukin-2 and Interleukin-12 Combine with Radiation Therapy to Safely Potentiate Regression of Advanced Malignant Melanoma in Pet Dogs

Citation: Jordan A. Stinson, Matheus Moreno P. Barbosa, Allison Sheen, Noor Momin, Elizabeth Fink, Jordan Hampel, Kim A. Selting, Rebecca L. Kamerer, Keith L. Bailey, Karl D. Wittrup, Timothy M. Fan; Tumor-Localized Interleukin-2 and Interleukin-12 Combine with Radiation Therapy to Safely Potentiate Regression of Advanced Malignant Melanoma in Pet Dogs. Clin Cancer Res 15 September 2024; 30 (18): 4029–4043.

Published Version: 10.1158/1078-0432.ccr-24-0861

Publisher: American Association for Cancer Research

Permanent Link: https://hdl.handle.net/1721.1/164939

Version: Final published version: final published article, as it appeared in a journal, conference proceedings, or other formally published context

Tumor-Localized Interleukin-2 and Interleukin-12 Combine with Radiation Therapy to Safely Potentiate Regression of Advanced Malignant Melanoma in Pet Dogs

Jordan A. Stinson[1,2], Matheus Moreno P. Barbosa[3], Allison Sheen[1,2], Noor Momin[1,2,4], Elizabeth Fink[1,5], Jordan Hampel[3], Kim A. Selting[3], Rebecca L. Kamerer[3], Keith L. Bailey[6], Karl D. Wittrup[1,2,5], and Timothy M. Fan[3,7]

ABSTRACT

Purpose: Cytokines IL2 and IL12 exhibit potent anticancer activity but suffer a narrow therapeutic window due to off-tumor immune cell activation. Engineering cytokines with the ability to bind and associate with tumor collagen after intratumoral injection potentiated response without toxicity in mice and was previously safe in pet dogs with sarcoma. Here, we sought to test the efficacy of this approach in dogs with advanced melanoma.

Patients and Methods: This study examined 15 client-owned dogs with histologically or cytologically confirmed malignant melanoma that received a single 9-Gy fraction of radiotherapy, followed by six cycles of combined collagen-anchored IL2 and IL12 therapy every 2 weeks. Cytokine dosing followed a 3 + 3 dose escalation design, with the initial cytokine dose chosen from prior evaluation in canine sarcomas. No exclusion criteria for tumor stage or metastatic burden, age, weight, or neuter status were applied for this trial.

Results: Median survival regardless of the tumor stage or dose level was 256 days, and 10/13 (76.9%) dogs that completed treatment had CT-measured tumor regression at the treated lesion. In dogs with metastatic disease, 8/13 (61.5%) had partial responses across their combined lesions, which is evidence of locoregional response. Profiling by NanoString of treatment-resistant dogs revealed that *B2m* loss was predictive of poor response to this therapy.

Conclusions: Collectively, these results confirm the ability of locally administered tumor-anchored cytokines to potentiate responses at regional disease sites when combined with radiation. This evidence supports the clinical translation of this approach and highlights the utility of comparative investigation in canine cancers.

Introduction

The recent success of immune checkpoint inhibitors has ushered in a new era to treat advanced cancers through rational engagement of the immune system (1–3). Remarkable objective responses have been observed in primary tumors across a multitude of cancer immunotherapy strategies, although achievement of objective responses at metastatic sites remains an elusive clinical outcome for the majority of patients (4–6). As such, combinations of checkpoint inhibitors with immune agonists have been explored to enhance systemic antitumor responses by overcoming immune-suppressive barriers operative at these metastatic sites (7, 8). In particular, the cytokines IL2 and IL12 have garnered significant interest owing to their ability to proliferate, activate, and differentiate critical effector immune cell populations unleashed by checkpoint inhibitors (9, 10). Encouraging synergy has been observed with these IL/checkpoint inhibitor combinations in early clinical trials, although adverse side effects have been encountered in patients (11–13). As key signaling molecules between immune cells, endogenous immune-stimulating cytokines like IL2 and IL12 exhibit tightly controlled spatial distributions and diffusional kinetics to prevent aberrant and pathologic activation. However, in the therapeutic setting, systemically dosed cytokines can elicit on-target, off-tumor activation of immune cells and subsequently possess an extremely narrow therapeutic window constrained by dose-limiting toxicities (14–16). These clinical limitations resulting from systemically administered cytokines have driven the recent interest in protein engineering strategies to mitigate systemic toxicities through tumor-targeting immunocytokines (17–21), conditionally active/masked cytokines (22–26), and receptor-biased cytokine agonists (27–30) to enable their inclusivity alongside checkpoint inhibitors and other first-line cancer treatments such as radiation, chemotherapy, and surgery.

These elegant protein engineering efforts converge on the same objective for cytokine therapies that promote their accumulation within the tumor and constrain their signaling to the immediate tumor microenvironment. With advances in image-guided injection techniques, intratumoral dosing of therapies is now possible for the majority of solid tumor indications. As such, we and others have begun to explore strategies to physically retain cytokines like IL2

[1]Koch Institute for Integrative Cancer Research, Massachusetts Institute of Technology, Cambridge, Massachusetts. [2]Department of Biological Engineering, Massachusetts Institute of Technology, Cambridge, Massachusetts. [3]Department of Veterinary Clinical Medicine, University of Illinois at Urbana-Champaign, Urbana, Illinois. [4]Department of Bioengineering, University of Pennsylvania, Philadelphia, Pennsylvania. [5]Department of Chemical Engineering, Massachusetts Institute of Technology, Cambridge, Massachusetts. [6]Alnylam Pharmaceuticals, Inc., Cambridge, Massachusetts. [7]Cancer Center at Illinois, University of Illinois at Urbana-Champaign, Urbana, Illinois.

J.A. Stinson and M.M.P. Barbosa contributed equally to this article.

K.D. Wittrup and T.M. Fan are co-senior authors to this work.

Corresponding Authors: Timothy M. Fan, Department of Veterinary Clinical Medicine, University of Illinois Urbana-Champaign, Urbana, IL 61820. E-mail: t-fan@illinois.edu; and Karl D. Wittrup, Department of Chemical and Biological Engineering, Massachusetts Institute of Technology, Cambridge, MA 02139. E-mail: wittrup@mit.edu

Clin Cancer Res 2024;30:4029–43

doi: 10.1158/1078-0432.CCR-24-0861

Translational Relevance

In the era of immunotherapy, the translation of immune-modulating strategies requires the inclusion of model systems that faithfully recapitulate the complex and reactive tumor microenvironment. Immunocompetent pet dogs with naturally occurring cancers can serve as high-value translational links between mouse and human studies. Canine tumors share key characteristics with human cancers including immune evasion mechanisms and genetic diversity. Additionally, pet dogs often present with regional and/or distant metastatic disease, enabling the assessment of abscopal responses to innovative localized therapies. Building upon our previous work on tumor microenvironment reprogramming with intratumoral collagen-anchored cytokines, herein we explore anticancer activities of a prime-boost treatment strategy inclusive of intratumoral cytokines and radiotherapy in pet dogs with advanced melanoma. Provocatively, we document robust anticancer activities, supporting the investigation of engineered anchoring cytokines in human patients with cancer, and our results underscore the value for a comparative oncology approach to inform the design of human clinical studies.

and IL12 within the tumor microenvironment after intratumoral injection through binding to co-dosed biomaterials (31–34) or extracellular matrix components like collagen (25, 35–37). These approaches minimize the systemic biodistribution, tumor accumulation, and toxicity challenges associated with systemic dosing of engineered cytokines and have led to marked improvements in both safety and efficacy profiles versus non-retained cytokines in mouse tumor models (31, 35, 36). However, mouse syngeneic transplant tumor models lack the long-term immune selection pressures that sculpt human tumor genetics, and thus they incompletely recapitulate critical evolutionary features of the complex human tumor microenvironment (38, 39). As a result, the achievement of treatment efficacy in mouse preclinical models with investigational immunotherapies is not sufficient for predicting their success when translated to human clinical trials (40–42). For this reason, naturally occurring tumors in larger companion animals complement these conventional model systems by illuminating the nuanced and complex tumor–immune interactions otherwise undetectable in mouse tumors, aiding translational investigation of novel anticancer strategies.

Here, we build upon our prior work in murine tumor models by examining the safety and efficacy of intratumorally delivered, collagen-retained IL2 and IL12 cytokines in advanced malignant melanomas that spontaneously develop in outbred pet dogs. Dogs develop cancer at similar rates to humans and yet are an underutilized model to bridge the gaps between mouse and human studies of novel immunotherapies or treatment combinations (43–45). Canine tumors feature many of the same biological immune escape mechanisms and intratumor genetic heterogeneity that define human cancers, while also possessing more human-relevant body characteristics that enable the prediction of drug biodistribution and pharmacokinetics/pharmacodynamics (46–49). Canine malignant melanomas typically feature mutational burden at >1 mutation/Mb, with mutational enrichment across the p53 and RAS signaling pathways (50). Moreover, a significant fraction of pet dogs with cancer presents with metastatic disease, enabling the evaluation of locoregional response to intratumoral therapy, which has been far more difficult to model and test in murine tumors or genetically engineered mouse models. We previously evaluated the safety and mechanism of action of an intratumoral collagen-binding cytokine approach in canine soft-tissue sarcomas but did not have the opportunity to investigate long-term antitumor responses due to the medical ethical obligation to resect such tumors shortly after treatment (51). Guided by palliative regimens for malignant melanoma using hypofractionated radiotherapy (RT), we here report our studies of the safety and efficacy of a single RT dose with repeat dosing of tumor-localized IL2 and IL12 cytokines against malignant melanoma, a canine cancer that metastasizes in more than 70% of cases (52). Through a dose-escalation trial inclusive of key immunobiological endpoints, we observed provocative activity engendered at both primary and metastatic tumors in a defined cohort of pet dogs. Profiling of canine patients that progress after therapy inform hypotheses regarding new therapeutic combinations predicted to improve tumor response rates, and we intend to deploy these strategies in both mouse models and pet dogs with naturally occurring cancers. Collectively, these efforts underscore the potential utility of comparative oncology inclusive of canine tumors to build, test, and optimize treatment regimens prior to commencing human clinical studies.

Patients and Methods

Ethics statement

This study complies with all relevant ethical norms and principles. This research study protocol was approved by the Institutional Animal Care and Use Committee (IACUC) at the University of Illinois Urbana-Champaign (UIUC), and this study was conducted in accordance with the ARRIVE guidelines.

Trial eligibility and enrollment of pet dogs

Client-owned pet dogs with cytologically or histologically confirmed oral malignant melanoma (OMM) were included in the study (**Table 1**). Eligibility criteria required the dogs to have (i) primary tumor measure between 0.5 and 7.5 cm in diameter, (ii) adequate organ function determined by laboratory evaluations (complete blood count, serum biochemical profile, and urinalysis), and (iii) a minimum 3-week washout period for RT, systemic chemotherapy, or any additional immunosuppressive/homeopathic/alternative therapy. No exclusion criteria for tumor stage or metastatic burden, age, weight, sex, or neuter status were applied for this trial. Tumor staging at enrollment was determined on the basis of the World Health Organization (WHO) staging scheme for dogs with oral melanoma (Supplementary Table S1; ref. 53). All patient owners provided written informed consent before enrollment, and all procedures were performed in accordance with the study protocol approved by the UIUC IACUC.

Collagen-anchoring IL2 and IL12 cytokine protein production

Canine cytokines (cLAIR-CSA-cIL2 and cIL12-CSA-cLAIR) were cloned and recombinantly expressed as previously described (51). Briefly, HEK293-F (Gibco; RRID: CVCL_D603) stable cell lines for each cytokine were prepared through cloning into the expression cassette of PiggyBac (System Biosciences) transposon vector, followed by dual transfection of the transposon vector and the Super PiggyBac transposase plasmid. Stable integration was confirmed after sorting enhanced green fluorescent protein–positive cells 3 to

Table 1. Dosing information and baseline patient characteristics.

	Cohort 1×	Cohort 2×	Cohort 3.3×	Cohort 5×	Total
	(*n* = 3)	(*n* = 6)	(*n* = 4)	(*n* = 2)	(*n* = 15)
Dosing information					
LAIR-CSA-IL2 dose ("IL2"; μg/kg)	17.4	34.8	57.4	87.0	80 doses
IL12-CSA-LAIR dose ("IL12"; μg/kg)	2.08	4.16	6.86	10.4	80 doses
Breed					
Purebred					
Miniature Schnauzer	1 (33%)	—	—	—	1 (6.7%)
German Shepard	1 (33%)	—	—	—	1 (6.7%)
German Shorthaired Pointer	—	1 (16.6%)	—	—	1 (6.7%)
Labrador Retriever	—	1 (16.6%)	1 (25%)	1 (50%)	3 (20%)
Dachshund	—	—	1 (25%)	—	1 (6.7%)
Yorkshire Terrier	—	—	1 (25%)	—	1 (6.7%)
Shih Tzu	—	1 (16.6%)	—	—	1 (6.7%)
Standard Poodle	—	—	—	1 (50%)	1 (6.7%)
Australian Cattle Dog	—	—	1 (25%)	—	1 (6.7%)
Mixed breed	1 (33%)	3 (50%)	—	—	4 (26.7%)
Primary site of malignant melanoma, *n* (%)					
Lip/buccal mucosa	—	2 (33%)	—	1 (50%)	3 (20%)
Mandible/mandibular mucosa	1 (33%)	3 (50%)	1 (25%)	—	5 (33.3%)
Maxilla/maxillary mucosa	1 (33%)	1 (17%)	3 (75%)	1 (50%)	6 (40%)
Periocular	1 (33%)	—	—	—	1 (16.7%)
Age (years)					
Median (min, max)	11 (4, 13)	11.5 (8, 16)	10.5 (7, 12)	10.5 (10, 11)	11 (4, 16)
Baseline weight (kg)					
Median (min, max)	23.2 (5.8, 33.2)	16.5 (6.8, 33.9)	12.8 (4.7, 31.8)	34.9 (29.3, 40.4)	21.2 (4.7, 40.4)
Baseline tumor volume (cm^3)					
Median (min, max)	7.5 (4.7, 11.6)	6.8 (0.5, 16.3)	7.9 (2.7, 18.6)	23.2 (3.0, 43.4)	7.5 (0.5, 43.4)
Baseline WHO stage, *n* (%)					
I	—	1 (17%)	—	—	1 (6.7%)
II	1 (33%)	2 (33%)	1 (25%)	—	4 (26.7%)
III	1 (33%)	2 (33%)	2 (50%)	—	5 (33%)
IV	1 (33%)	1 (17%)	1 (25%)	2 (100%)	5 (33%)

NOTE: Description and dosing group allocation of 15 canine patients enrolled in the study. Patient breed, age, weight, tumor location, initial volume, and WHO domestic animal tumor stage are reported.

4 days after transfection (BD FACSAria), and transformed HEK293-F cell lines were confirmed to be mycoplasma free (IDEXX RADIL). Protein was produced from IL2- and IL12-expressing stable lines during 1-week culture in serum-free media (FreeStyle 293, Invitrogen) and purified with HisPur Ni-NTA affinity resin (Thermo Fisher Scientific). Protein was analyzed by using size exclusion chromatography (Superdex 200 Increase 10/300 GL column, Cytiva Life Sciences, on ÄKTA FPLC system) for size and aggregation and validated to meet low endotoxin levels (<5 EU/kg) by using the Endosafe nexgen-PTS system (Charles River Laboratories). Activity of cytokines was confirmed through CTLL2 and HEK Blue IL12 activation assays, while collagen-binding was confirmed through ELISA. Both CTLL2 (ATCC, Cat# TIB-214, RRID: CVCL_0227) and HEK-Blue IL12 (InvivoGen; RRID: CVCL_UF31) cells were cultured according to the vendor's instructions in 5% CO_2 at 37°C. These cells also tested negative for mycoplasma. Aliquots of cytokines were snap-frozen in liquid nitrogen and thawed immediately prior to dilution in sterile saline for dosing intratumorally to dogs.

Study design and intratumoral dosing of cytokines

Fifteen eligible dogs were enrolled into a modified Fibonacci 3 + 3 dose escalation trial design of four different cohorts. The trial consisted of a regimen involving treatment with a single 9-Gy dose of RT followed by six doses of cLAIR-CSA-cIL2 (IL2) and cLAIR-CSA-cIL12 (IL12) every 2 weeks. Radiation was delivered using a Varian TrueBeam linear accelerator with 6 MV photons at standard dose rate of 6 Gy/minute (Varian Medical Systems, Palo Alto, CA). Depending on the location and proximate organs at risk, the dose was delivered either using manual calculations for parallel opposed portals or with three-dimensional conformal radiation plan using CT guidance and a treatment planning system (Varian Eclipse v.15). The dose was calculated to the central axis for parallel opposed portals and with the goal of 100% of dose to 95% of the planning target volume (gross tumor volume plus a 3 to 5 mm expansion) for computer plans. The initial doses of IL2 and IL12 cytokines used in this work were determined from prior evaluation in both healthy beagles and pet dogs with soft-tissue sarcomas (51). The reported values for single-agent maximum tolerated doses (MTD) of IL2 in humans (54–56) and IL12 immunocytokine in dogs (57) were used to select the maximum cytokine dose in our prior work, with the "1×" dose level described here representing 0.1× the MTD (Supplementary Table S2). Doses of cLAIR-CSA-cIL2 (17.4 μg/kg at "1×" dose level) and cIL12-CSA-cLAIR (2.08 μg/kg at "1× dose level") were prepared from frozen protein aliquots and combined in

a total volume not exceeding 0.5 mL in sterile saline. A 29-gauge, 0.5-inch insulin syringe was used to slowly inject the full dose volume via a single insertion point using a fanning pattern into the tumor. No additional measures were used to avoid any internal necrotic areas within the tumor. Radiation therapy was performed using the Varian TrueBeam system. Adverse events were classified and graded in accordance with the Veterinary Cooperative Oncology Group's Common Terminology Criteria for Adverse Events (v2; ref. 58). An additional cohort of three dogs was recruited to examine the response to IL2/IL12 cytokine-only dosing. Three other dogs undergoing RT for their oral melanoma consented to blood draws following administration of radiation to examine circulating cytokine/chemokine biomarkers as the control cohort. These patients undergoing RT-only were not followed for survival analyses.

Clinical response assessment

Clinical and vital evaluations were conducted on all patients at baseline and preceding each treatment administration at the UIUC Veterinary Teaching Hospital. In addition, after intratumoral cytokine administration, a 48-hour monitoring period was initiated to assess the presence of any toxicity-related symptoms, coupled with blood sampling for complete blood count, serum biochemical profiling, and urinalysis. In addition, after each treatment, blood draws by jugular venipuncture were performed for cytokine/chemokine analysis before treatment and at 2, 4, 8, 24, and 48 hours after treatment. Patients were followed up until their death or removal from the trial.

Clinical and caliper measurements of the maximum tumor and lymph node dimensions were conducted by board-certified veterinary oncologists, and measurements were documented in millimeters during each examination. In addition, primary tumor or metastatic lesions were assessed by CT (SOMATOM Definition AS, Siemens Healthineers) at pretreatment, day 28, day 70, and day 84 (2 weeks after the last treatment). The tumor size and percentage of change were determined on the basis of CT measurements. Because determination of the longest dimension is challenging with these frequently irregularly marginated tumors, the tumor volume was used to measure the response to therapy. Volume was determined using the RT treatment planning software (Eclipse v15, Varian, Palo Alto, CA) by importing CT scan images (1.5-mm slices) before and after treatment. The gross tumor volume was delineated on the basis of distortion of normal tissues by the mass effect combined with changes in Hounsfield units, which reflect contrast enhancement due to changes in electron density. The software yields a three-dimensional volume based on the contours that are created. Standard criteria for volumetric assessment of tumor response were used. Furthermore, the assessment of tumor response was carried out during each visit and was determined in accordance with the guidelines established by the RECIST in Dogs (v1.0; Veterinary Cooperative Oncology Group; ref. 59). These guidelines similarly reflect the human RECIST v1.1 response criteria in the assessment of canine tumors: complete response (resolution of all target lesions and no new lesions), partial remission (at least 30% reduction in target lesions and no new lesions), stable disease (SD; no more than 20% increase in target lesions or a decrease in target lesions less than 30% and no new lesions), or progressive disease (PD; >20% increase in target lesions and new lesions). Patients presenting with SD or PD were allowed to remain in the study under the condition that no adverse events were observed or if such events could be mitigated through the implementation of a dose reduction protocol. Clients had the option to remove their dogs from the study if their pets' conditions worsened, if they showed signs of declining health, or if the treatment caused unbearable side effects. The decision could be made by the investigator, the dog's owner, or both.

Multiplex cytokine assay and ELISA

Serum samples collected from patients following treatment were examined for concentrations of 13 cytokine and chemokine analytes, including GM-CSF, IFNγ, IL2, IL6, IL7, IL8/CXCL8, IL10, IL15, IL18, IP10/ CXCL10, KC-like, MCP1/CCL2, and TNFα (MILLIPLEX Canine Magnetic Bead Panel, Millipore Sigma) at Eve Technologies (Calgary, AB, Canada). Individual analyte concentrations were determined from panel standard curves for each cytokine or chemokine. Time course analysis of patient response to IL2/IL12 and RT was performed by determining the $\log_{10}$ fold change of analyte concentrations relative to their pretreatment levels. IFNγ and IL10 serum concentrations following treatment with collagen-anchored cytokines and RT were further measured using the Canine IFNγ Quantikine ELISA Kit (R&D Systems) and the Canine IL10 Quantikine ELISA Kit (R&D Systems) according to the manufacturer's instructions.

NanoString RNA profiling

RNA was isolated from 10-μm formalin-fixed, paraffin-embedded (FFPE) samples from resected canine primary melanoma tumor or metastatic tumor lesions using an RNEasy FFPE Kit and deparaffinization solution (QIAGEN). Isolated RNA was examined by using Bioanalyzer (Agilent) for the assessment of fragment size prior to hybridization with nCounter probe sets (NanoString). Canine RNA samples were hybridized with the Canine IO nCounter Panel code set for 22 hours at 65°C per the manufacturer's instructions. Following hybridization, the samples were loaded into the analysis cartridge and scanned at maximum resolution using NanoString Prep Station and Digital Analyzer.

Canine RCC count files were normalized using nSolver software (NanoString) after background thresholding using the mean of eight negative control probes and batch correction against a standard control panel. Normalized gene counts were processed using the nSolver Advanced Analysis module for differential expression and pathway enrichment analysis. *P* value adjustment was performed using the Benjamini–Hochberg method to estimate FDRs of differentially expressed genes.

Estimation of tumor immune cell abundance

Relative abundance of the tumor-infiltrating cell fraction was estimated from bulk NanoString profiling data by employing CIBERSORTx (60) algorithm using a validated leukocyte gene signature matrix (LM22). Bulk NanoString profiling data were assessed in relative mode, with 100 permutation runs and without quantile normalization.

Immunohistochemistry and cytology

Canine advanced malignant melanoma tumors were resected at specific indicated timepoints. Following resection, tumor tissues were fixed in 10% formalin and subjected to a paraffin processing and embedding protocol. IHC was used to determine the presence of inflammatory cells, specifically positive for CD3 (T lymphocyte; Biocare, CP215C), Iba-1 (macrophage; Biocare, Cat# CP 290 B, RRID: AB_10583150), and Melan-A (melanoma-specific antigen; Biocare, A103) for melanoma cells. All samples were histologically evaluated and classified by a single board-certified veterinary pathologist. Tumor tissues were classified based on CD3 T-cell

infiltration status into an immune phenotype, defined as (i) inflamed—highly infiltrated by $CD3^+$ T cells, (ii) immune desert/cold—devoid of $CD3^+$ T cells, and (iii) immune excluded—bordered yet not infiltrated by $CD3^+$ T cells (61). Cytology of tumors was performed at specified timepoints. Cellular specimens were collected using a 22-gauge needle attached to a 5-mL syringe. Following aspiration, the samples were smeared onto a glass slide for subsequent cytochemical staining. Cytology slides were then evaluated by a board-certified veterinary pathologist. IHC staining and cytology samples were assessed on an Olympus BX45 microscope using a high-power 10× microscope objective. Digital images were captured with an Olympus DP28 digital camera and processed using Olympus cellSens Imaging Software (v4.2).

Statistical analysis

Statistical analyses were conducted using Prism v10 (GraphPad, RRID: SCR_002798). Power calculations were not conducted to predetermine sample size. The details of statistical analysis have been provided in the descriptions for **Figs. 2** and **4**.

Data availability

The data generated in this study are available within the article and its supplementary files (Supplementary Data S1), and the raw data generated are available from the corresponding author upon reasonable request. NanoString expression data for canine tumor expression in dogs progressing after completion of RT with the IL2 and IL12 therapy has been made publicly available in Gene Expression Omnibus (RRID:SCR_005012) at GSE253243.

Results

Patient enrollment and study population

For this study, clients whose dogs met the trial inclusion criteria provided written informed consent before enrollment, and all procedures were performed in accordance with the study protocol approved by the UIUC IACUC. The dogs were eligible after histologic or cytologic confirmation of OMM ($n = 14$) or malignant melanoma involving other facial structures ($n = 1$) and if their primary tumor was between 0.5 and 7.5 cm in diameter. Eligible dogs were also required to have adequate organ function as measured by standard laboratory tests and have had a minimum 3-week washout period if they had been recently treated with RT, systemic chemotherapy, immunotherapy, or any additional homeopathic/alternative therapy. There were no exclusion criteria for tumor stage or metastatic burden, age, weight, sex, breed, or neuter status for this study. Dogs were sequentially enrolled into a modified Fibonacci 3 + 3 dose escalation trial design, with the initial IL2 and IL12 cytokine dose chosen from prior identification of an MTD after evaluation in both healthy beagles and pet dogs with soft-tissue sarcomas (**Table 1**; ref. 51). The low dose level ("1×") tested here represented one-tenth the MTD identified in a prior work (51), which was informed by a reported IL12 immunocytokine MTD in dogs (57) and allometric scaling of single-agent IL2 doses in humans (Supplementary Table S2; refs. 54–56). In total, 15 dogs with median age 11 years (min: 4, max: 16) were enrolled into the trial, with 10/15 (66%) dogs presenting with tumors of World Health Organization stage III or greater, indicating metastatic disease at lymph nodes or lung tissue sites (Supplementary Table S1).

Tumor-localized IL2/IL12 with radiation is effective against canine oral melanoma

The primary objective of this study was to examine the antitumor efficacy potentiated by the combination of intratumoral collagen-anchored IL2 and IL12 with a single dose of RT. As current veterinary practice patterns favor the use of hypofractionated RT protocols using 8 to 10 Gy fraction size for OMM (62–64), dogs treated in this study were provided a single RT dose of 9 Gy to stimulate tumor cell death and antigen generation. Local and regional lymph nodes were not irradiated, regardless of appearance or suspicion of possible metastatic disease. Dogs then received six doses of intratumoral collagen-anchored cytokines at the same 2-week cadence similar to an existing FDA-approved intratumoral immune strategy [e.g., Talimogene laherparepvec (T-VEC); **Fig. 1A**]. Pursuit of consecutive additional RT doses was not instituted because of concerns for detrimental lymphodepletion within the tumor and draining lymph node following preliminary experiments in the murine B16F10 model and other reports (Supplementary Fig. S1A–G; refs. 65–67). Moreover, the subsequent dosing of intratumoral cytokine alone enabled attribution of patient symptoms uniquely to cytokine treatment and bypassed the requirement to deconvolute individual or interactive toxicities generated by continuous combinatorial therapy of RT with IL2 and IL12. All dogs were monitored for 48 hours after intratumoral cytokine dosing for symptoms of toxicity and had periodic blood draws performed for cellular and chemistry analyses.

Primary tumor volumes at the time of the first intratumoral dose had a median volume of 7.5 cm^3 (min: 0.5, max: 43.4), although the highest dose cohort ("5×") included a dog with a primary tumor volume near the upper end of our eligibility criteria (**Fig. 1B**). Responses to therapy were evaluated through comparative and serial assessments of CT scans of primary tumor and associated regional metastatic lymph nodes identified at the baseline (pretreatment) with subsequent CT scans performed on day 28 and day 84. Rapid primary tumor volume reduction occurred in 13/15 (86.7%) malignant melanomas at day 28 scan after just two doses of cytokine therapy and a single RT dose (**Fig. 1C**). At day 84 CT scan, performed 2 weeks after the final (sixth) dose of intratumoral cytokine treatment, primary tumor responses were found to be stable or have further improved in 10/13 (76.9%) surviving dogs (**Fig. 1D**). Two patients were euthanized before the day 84 CT tumor measurement because of progression of their primary and/or metastatic tumor sites. These tissues were collected for additional analysis, which is detailed later in this study.

Treated pet dogs were followed after the 12-week treatment period to monitor the durability of their responses and assess overall survival. As of the time of writing (January 2024), the median survival regardless of tumor stage is 256 days, with three dogs still alive the past 2 years (**Fig. 1E**; Supplementary Fig. S2A and S2B). This is in contrast to the reported median survival of 65 days for dogs with untreated oral melanoma (68) and 147 days for OMM dogs treated with 9 Gy × 4 RT (63). Two dogs were euthanized because of unrelated issues (age/quality of life; development of sinonasal chondrosarcoma) nearly a year after completing treatment. Interestingly, there appeared to be no correlation between the cytokine dose level and overall survival (Supplementary Fig. S3A–D). Of the dogs alive nearly 1,000 days after treatment, the local response to therapy was rapid and robust, with less treatment morbidity than curative-intent surgical removal of OMM (**Fig. 1F** and **G**). Overall, the objective responses observed in these canine patients with advanced stage and heterogeneous primary tumors were favorable, and further corroborate and extend upon the documented anticancer activities demonstrated in mouse models treated with the same collagen-binding cytokine approach (35, 37).

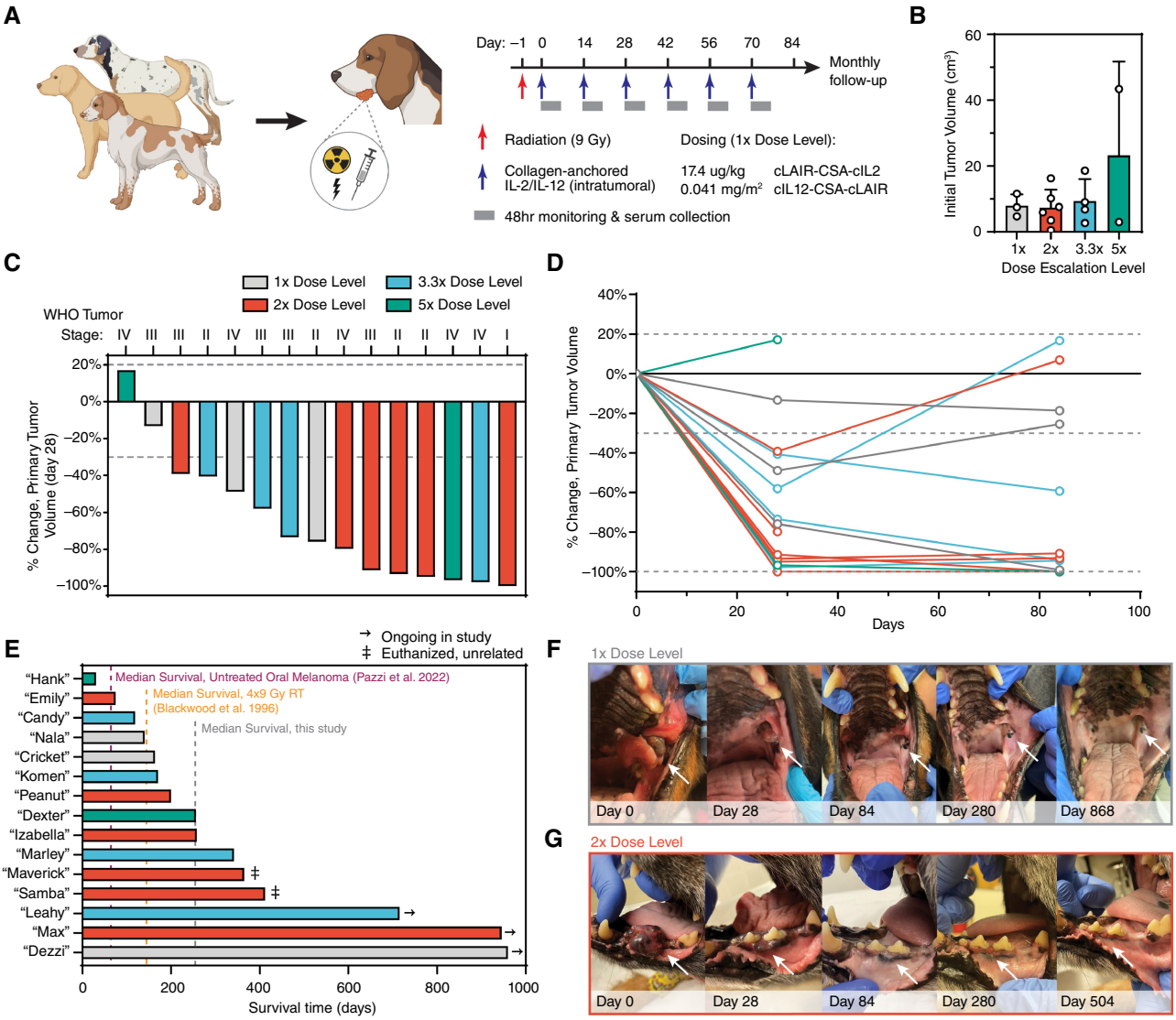

Figure 1.

Study design and treatment outcomes. **A,** Study-eligible dogs received 9 Gy of radiation (red arrow) followed by six doses of intratumorally administered cytokines (blue arrows). Each cytokine dose was followed by 48 hours of clinical monitoring and serum collection. **B,** Pretreatment primary tumor size quantified via CT radiologic assessment. **C,** Percent change in tumor volume after radiation and two doses of intratumorally administered cytokines. Dotted lines depict RECIST criteria for tumor progression or clinical response. **D,** Percent change in primary tumor volume during the course of treatment with intratumorally administered cytokines. One patient in each of the 2× and 5× dosing cohorts was euthanized prior to day 84 due to outgrowth of metastatic or primary tumors. **E,** Swimmer plot of length of patient survival after trial start. **F** and **G,** Images of primary tumors taken at indicated time points from select dogs from the 1× (**F**) and 2× (**G**) cohorts who displayed durable and complete response to treatment. (**A,** Created with BioRender.com).

Effective intratumoral doses of IL2/IL12 are also safe in pet dogs

The clinical promise of IL2 and IL12 cytokines has been limited by the toxicities observed at therapeutically effective doses (9, 10, 15, 16, 69, 70). As such, evaluating if the collagen-anchoring approach would ameliorate cytokine-driven toxicities at doses capable of promoting antitumor responses in pet dogs was paramount and translationally relevant. Analysis of whole blood at intervals following the first and second doses of intratumoral cytokine therapy indicated minimal elevation of systemic alanine transaminase (ALT) levels for most patients tested at the lowest three dose levels, with ALT levels normalizing prior to administration of each subsequent cytokine dose (**Fig. 2A**). The predominant adverse events observed were mostly grade 1 and 2 across dose-level cohorts, with the most commonly occurring events being associated with hemoglobinemia, thrombocytopenia, lethargy, anorexia, and elevation in ALT and alkaline phosphatase (ALP) levels (**Table 2**). The owner of one 2×-dose-level dog with elevated ALT chose not to pursue the sixth dose of cytokine treatment. Select dogs demonstrated elevated ALT in the 3.3× dose cohort and responded well to s-adenosylmethionine and

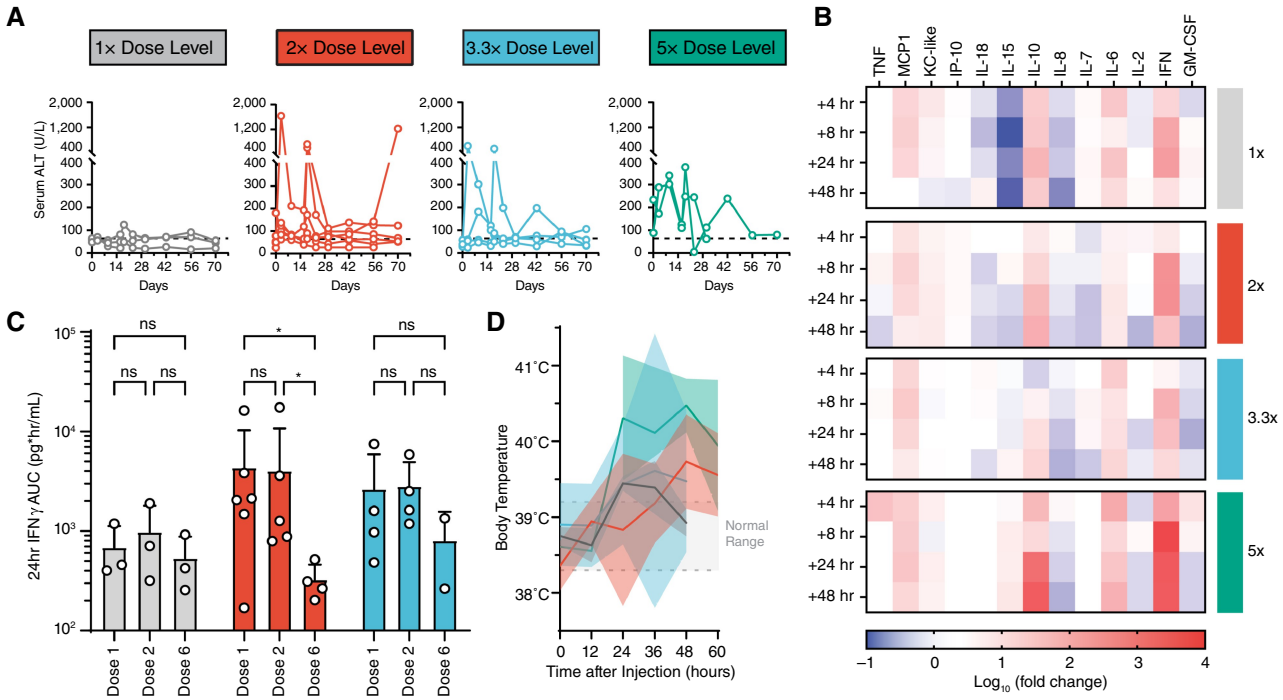

Figure 2.

Safety profile of collagen-anchored cytokine therapy. **A,** Serum ALT levels measured via blood work at indicated time points following intratumoral cytokine dosing at day 0 and day 14. Dotted line indicates a clinically healthy ALT threshold. **B,** Serum was collected at several time points after the first intratumoral cytokine injection and analyzed for cytokines and chemokines. Heatmap rows describe averaged sera data from each dosing cohort, reported as $\log_{10}$ fold change in concentration compared with pretreatment values. **C,** Serum was collected 4, 8, and 24 hours after cytokine administration after the indicated doses and analyzed for systemic exposure to IFNγ, as represented by 24 hours IFNγ AUC. **D,** Body temperature of patients was measured at the indicated time points after the first cytokine administration. Dotted lines indicate normal body temperature range. Statistics: IFNγ AUCs compared by two-way ANOVA with Tukey multiple comparisons test. *, $P < 0.05$. ns, not significant.

silybin to mitigate hepatocyte toxicity and normalize liver function. More clinically significant ALT elevation and symptoms consistent with cytokine release syndrome (i.e., thrombocytopenia, hypoproteinemia, severe lethargy, and pyrexia) were observed in the 5× dose cohort (**Table 2**). These patients received supportive care including intravenous fluids and dexamethasone SP (0.5 mg/kg, IV) and fully recovered after treatment. A reduction in subsequent doses to this cohort to 3.3× was instituted to minimize discomfort and health risks in these patients.

To correlate the observed clinical activity and potential toxicity with pharmacodynamic biomarkers, profiling of the systemic chemokine/cytokine responses to combination RT with intratumoral cytokine treatment was performed. Similar response dynamics to those previously reported were observed, wherein IL12 drives elevation of systemic levels of IFNγ, with a delay in the elevation of IL10 (**Fig. 2B**; refs. 51, 57, 71–73). Peak levels of IFNγ were mostly consistent among the lowest three dose cohorts, but spiked significantly higher at the more toxic 5× dose level. To confirm that circulating elevations of IFNγ and IL10 were biomarkers of intratumoral cytokine activities and not an epiphenomenon of ionizing radiation or injection site trauma, an additional cohort of four dogs receiving only a single dose of RT (9 Gy) and sham intratumoral saline injection was analyzed and no measurable concentrations of circulating IFNγ or IL10 was identified (Supplementary Fig. S4A–D). Moreover, a cohort of three dogs receiving intratumoral cytokine only without RT demonstrated similar dynamics of IFNγ and IL10 changes following treatment, providing further evidence that the dynamic responses observed via multiplex serum profiling are IL2/IL12 mediated rather than being due to the combination of RT with intratumoral cytokine treatment (Supplementary Fig. S4A–D). Biological antitumor responses were also observed in this cohort of dogs treated without radiation, demonstrating the critical role of IL2 and IL12 in potentiating regression of advanced melanoma in pet dogs (Supplementary Tables S3 and S4; Supplementary Fig. S5A and S5B).

Given the importance of IFNγ both directly on tumor cells and in facilitating productive antitumor immune responses (74–77), an estimation of the systemic exposure of patients to IFNγ via AUC was calculated. The analysis provided some evidence of immune tachyphylaxis, in which the response to intratumoral cytokine therapy seems to have diminished by the sixth dose, relative to the responses to the initial doses of therapy (**Fig. 2C**). This is most pronounced in the 2× dose cohort, although some pet owners elected to not continue treatment with six doses of intratumoral cytokine therapy because of complete regression of the local tumor site concurrent with some adverse toxicities [2/4 (50%) dogs], confounding the statistical comparisons at the 3.3× dose level. The phenomenon of immunologic defervescence has been difficult to study in murine models but has been noted in human patients, highlighting the potential utility to examine various treatment regimens in dogs to minimize tachyphylaxis. Characterization of antidrug antibody responses that could attenuate immunostimulatory

Table 2. Incidence of treatment-related adverse events.

	Cohort 1× (*n* = 3)					Cohort 2× (*n* = 6)					Cohort 3.3× (*n* = 4)					Cohort 5× (*n* = 2)					Total (*n* = 15)
Event	**Any grade**	**Grade 1**	**Grade 2**	**Grade 3**	**Grade 4**	**Any grade**	**Grade 1**	**Grade 2**	**Grade 3**	**Grade 4**	**Any grade**	**Grade 1**	**Grade 2**	**Grade 3**	**Grade 4**	**Any grade**	**Grade 1**	**Grade 2**	**Grade 3**	**Grade 4**	
Any event	40	33 (83%)	7 (17%)	0	0	168	93 (55%)	54 (32%)	18 (11%)	3 (1.8%)	122	84 (69%)	28 (23%)	10 (8.2%)	0	84	36 (43%)	31 (37%)	15 (18%)	2 (2.4%)	414 (100%)
Blood/bone marrow																					
Hemoglobinemia	5	5 (12.5%)	0	0	0	16	13 (7.7%)	2 (1.2%)	1 (0.6%)	0	14	11 (9%)	3 (2.5%)	0	0	8	7 (8.3%)	1 (1.2%)	0	0	43 (10.4%)
Thrombocytopenia	4	4 (10%)	0	0	0	12	10 (5.9%)	2 (1.2%)	0	0	11	8 (6.5%)	3 (2.5%)	0	0	6	2 (2.4%)	3 (3.6%)	0	1 (1.2%)	33 (8%)
Neutropenia	1	1 (2.5%)	0	0	0	0	0	0	0	0	0	0	0	0	0	0	0	0	0	0	1 (0.2%)
Lymphocytosis	0	0	0	0	0	1	0	1 (0.6%)	0	0	0	0	0	0	0	0	0	0	0	0	1 (0.2%)
Constitutional clinical signs																					
Fever	4	1 (2.5%)	3 (7.5%)	0	0	11	6 (3.6%)	5 (3%)	0	0	6	1 (0.8%)	3 (2.5%)	2 (1.6%)	0	4	0	3 (3.6%)	1 (1.2%)	0	25 (6%)
Lethargy/fatigue	6	5 (13%)	1 (2.5%)	0	0	8	6 (3.6%)	2 (1.2%)	0	0	14	10 (8.2%)	3 (2.5%)	1 (0.8%)	0	5	1 (1.2%)	3 (3.6%)	1 (1.2%)	0	33 (8%)
Dermatologic/skin																					
Edema (injected region)	1	0	1 (2.5%)	0	0	3	3 (1.8%)	0	0	0	4	3 (2.5%)	1 (0.8%)	0	0	2	2 (2.4%)	0	0	0	10 (2.4%)
Gastrointestinal																					
Diarrhea	3	3 (7.5%)	0	0	0	9	5 (3%)	3 (1.8%)	1 (0.6%)	0	2	2 (1.6%)	0	0	0	3	1 (1.2%)	2 (2.4%)	0	0	17 (4.1%)
Anorexia	4	4 (10%)	0	0	0	9	8 (4.8%)	1 (0.6%)	0	0	11	9 (7.4%)	1 (0.8%)	1 (0.8%)	0	6	3 (3.6%)	1 (1.2%)	2 (2.4%)	0	30 (7.2%)
Vomiting	0	0	0	0	0	0	0	0	0	0	2	2 (1.6%)	0	0	0	2	2 (2.4%)	0	0	0	4 (1%)
Dehydration	0	0	0	0	0	0	0	0	0	0	1	0	1 (0.8%)	0	0	0	0	0	0	0	1 (0.2%)
Metabolic																					
Increased ALT	7	6 (15%)	1 (2.5%)	0	0	43	16 (9.5%)	22 (13%)	2 (1.2%)	3 (1.8%)	17	10 (8.2%)	4 (3.3%)	3 (2.5%)	0	17	2 (2.4%)	10 (11.9%)	4 (4.7%)	1 (1.2%)	84 (20.3%)
Increased ALP	4	4 (10%)	0	0	0	33	8 (4.8%)	11 (6.5%)	14 (8.3%)	0	28	19 (16%)	6 (4.9%)	3 (2.5%)	0	16	6 (7.1%)	4 (4.7%)	6 (7.1%)	0	81 (19.6%)
Increased creatine phosphokinase	0	0	0	0	0	7	6 (3.6%)	1 (0.6%)	0	0	3	3 (2.5%)	0	0	0	4	4 (4.7%)	0	0	0	14 (3.4%)
Hypoalbuminemia	0	0	0	0	0	15	12 (7.1%)	3 (1.8%)	0	0	3	2 (1.6%)	1 (0.8%)	0	0	8	5 (5.9%)	3 (3.6%)	0	0	26 (6.3%)
Increased bilirubin	0	0	0	0	0	1	0	1 (0.6%)	0	0	4	3 (2.5%)	1 (0.8%)	0	0	3	1 (1.2%)	1 (1.2%)	1 (1.2%)	0	8 (2%)
Pain																					
Pain (injected region)	1	0	1 (2.5%)	0	0	0	0	0	0	0	2	1 (0.8%)	1 (0.8%)	0	0	0	0	0	0	0	3 (0.7%)

NOTE: Patients were clinically monitored for 48 hours after the administration of each dose of cytokine. Compiled grading of adverse events was performed in accordance with the Veterinary Cooperative Oncology Group's Common Terminology Criteria for Adverse Events (v2; ref. 58).

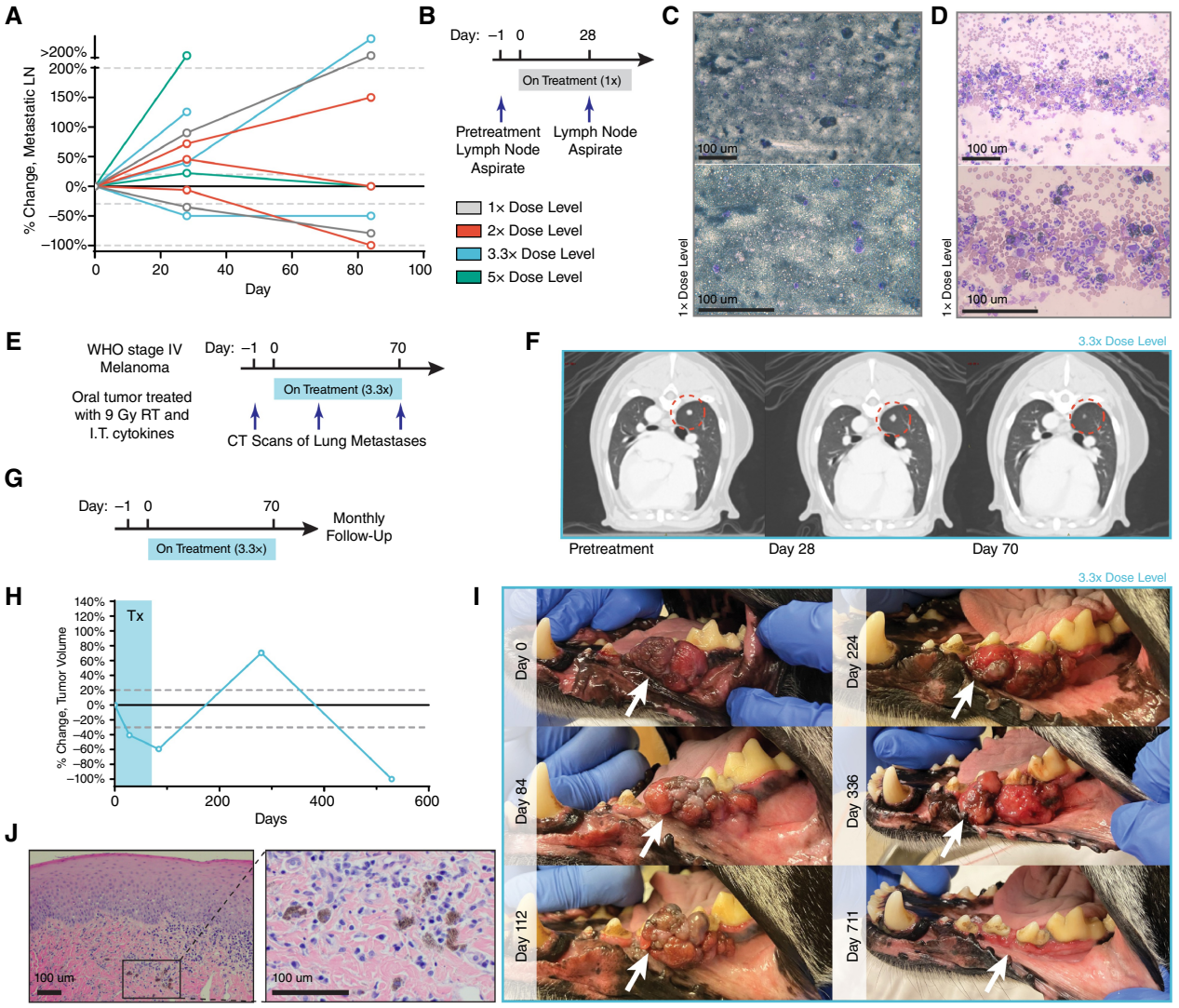

Figure 3.

Case studies of patients demonstrating abscopal immune responses. **A,** Percent change in volume of regional lymph node (LN) metastasis relative to pretreatment volume, as determined by CT measurement. **B,** Fine needle aspirate (FNA) was collected from the lymph node of a patient in the 1× cohort before treatment and after two intratumoral cytokine doses. **C,** Pretreatment aspirate shows diffuse infiltration of melanocytes. **D,** Lymph node disease is decreased after two cytokine treatments, with a marked increase in polymorphonuclear immune cells. **E,** CT images from a stage IV patient in the 3.3× treatment group were collected by tracking the progression of lung metastasis after local treatment of oral melanoma. **F,** CT images suggest pseudoprogression of lung metastasis after early cytokine doses, which later regressed after additional cytokine doses. **G–I,** A patient in the 3.3× dosing group received the full course of treatment and had routine follow-up visits to monitor tumor progression. Tumor measurements (**H**) and images (**I**) were taken at the indicated time points, demonstrating a significantly delayed treatment response. **J,** Hematoxylin and eosin staining on this tumor showed the absence of tumor cells with only scattered melanophages observed on day 529. Scale bars, 100 μm.

activities to collagen-anchored cytokines found the existence of antibodies but not at levels high enough to explain the magnitude of reduced IFNγ response at the final dose timepoint (Supplementary Fig. S6A–C).

Finally, patient body temperatures were measured during the posttreatment monitoring phase, and it was observed that most dogs became mildly febrile regardless of the dose level (**Fig. 2D**). These mild symptoms did not require medical intervention and were often accompanied by transient inappetence and lethargy among the patients during the monitoring phase. Overall, the responses potentiated by therapy were well tolerated at the 1× and 2× dose levels, with dose-limiting toxicities first observed at the 3.3× dose level in a subset of patients but among a majority of patients at 5×.

Tumor-localized IL2/IL12 with RT potentiates responses at metastatic lesions

Many pet dogs enrolled in this trial presented with metastatic lesions, providing an opportunity to examine whether local treatment of the primary tumor with IL2, IL12, and RT could promote

locoregional responses at untreated metastatic sites, an important outcome for intratumoral therapies. CT measurements were obtained for metastatic lymph nodes and measured for radiologic response in comparison with their pretreatment volumes (**Fig. 3A**). Following treatment of primary tumors with RT and intratumoral cytokines, 3/10 (30%) dogs displayed a partial response at metastatic lymph nodes. Two additional dogs achieved SD during the treatment period, for an overall biologic response rate to combination therapy in 5/10 (50%) dogs. Two dogs were euthanized prior to the day 84 measurement; one because of suspected progression of brain/CNS metastases and another for significant progression of lung metastases. For a subset of the responding patients, appreciable regional edema was present at metastatic lymph node sites at the interim (day 28) measurement.

For one patient, a pretreatment FNA of the tumor-draining lymph node and a subsequent FNA of the same regional lymph node in the day-28 CT scan were obtained (**Fig. 3B**). Prior to treatment, this lymph node was completely effaced with disease, as detected via the absence of immune cells and the majority presence of cancerous melanocytes and extracellular melanin (**Fig. 3C**). After two doses of intratumoral cytokine and single RT treatment, the lymph node CT scan indicated a robust decrease in metastatic regional lymph node volume (−35.3%; partial response) and concurrent immunologic clearing of melanoma cells and pigmentation (**Fig. 3D**). We observed the presence of polymorphonuclear cells, likely neutrophils, in the FNA, many of which had phagocytosed tumor cell debris and melanin. One additional patient had detectable lung metastasis at the time of presentation and trial enrollment (**Fig. 3E**). Although this dog ultimately succumbed to progressive metastatic disease, there was evidence of at least one regressing lung metastasis lesion during treatment (**Fig. 3F**). This mixed abscopal response may be due to underlying genetic differences between primary and disseminated disease, as well as among differing clonally derived lung metastases (78–80). However, the locoregional response of metastatic disease to combined intratumoral IL2/IL12 and single-dose RT treatment is consistent with an immune-mediated mechanism of action and similar to prior reports of combined radiation with immunotherapy (81–85).

Similar to the pivotal phase III clinical trials with T-VEC (86), out of concern that longitudinal sampling of the primary treated tumors could confound results by introducing additional paths for intratumoral dose egress, we did not profile the immune response to therapy during treatment. However, building upon our prior characterization of the immune-mediated response to collagen-anchored cytokines in canine soft-tissue sarcoma and murine tumors (35, 51), we highlight an anecdotal case of long-term antitumor response after the completion of treatment in oral melanoma which presumably involved immune activity.

One patient had a strong primary tumor response while on therapy but displayed slow growth of that tumor in the year following treatment completion (**Fig. 3G**). However, at the 12-month follow-up appointment after treatment, the primary tumor was no longer visible and was later confirmed to be absent via CT (**Fig. 3H** and **I**), as well as by histopathology (**Fig. 3J**). Additional immunohistochemistry for Melan-A further confirmed the absence of disease in the gingival tissue of this patient at day 529 (Supplementary Fig. S7). Although examples of spontaneous human tumor regressions have been reported (87, 88), they are quite rare ($\sim 10^{-5}$; ref. 87). The slow posttreatment tumor growth may correspond to a state of immune equilibrium, leading eventually to tumor elimination, similar to other immunotherapy approaches (89, 90).

Dysfunctional antigen presentation predicts resistance to tumor-localized cytokine therapy

Identifying and understanding which factors, if any, had contributed to poor response to the combined RT plus intratumoral cytokine treatment regimen was further studied. Toward this goal, FFPE-processed primary and metastatic tumor tissues from eight dogs that were euthanized for PD were advanced for detailed histologic and genomic evaluations. No clear trends were observed between the overall survival of these progressor patients and immune infiltration status profiled through immunohistochemistry for CD3 and Iba1 (Supplementary Fig. S8A–G). Extracted RNA from these tissue sections were profiled using the NanoString nCounter platform (**Fig. 4A**). A hierarchical cluster of pathway-specific gene expression emerged that encompassed the coordination of innate and adaptive immunity, including T-cell, B-cell, and macrophage functions, as well as antigen presentation (**Fig. 4B**). Within this cluster, varied expression among the progressor dogs was observed and additional unsupervised clustering of the antigen presentation gene set yielded two clusters of four dogs each (**Fig. 4C**). Given that tumor dysregulation of antigen presentation and response to IFNγ is a common immune evasion mechanism (75, 91, 92), the expression of MHC class I–related genes was examined and a significant difference in *B2m* and *Dla79* transcripts between the clusters of progressor dogs was identified (**Fig. 4D**). This result suggested that the first cluster of dogs may have had impaired MHC-I expression, at least among a partial population within the heterogeneous tumor. Broader comparisons in gene expression between these two cohorts indicated greater expression of effector lymphocyte-associated genes such as *Slamf6*, *Ctsw*, and *Trgc3*, as well as interferon-inducible genes such as *Ido1*, *Gbp5*, and *Cxcl10* among the MHC-I higher expression cohort, cluster 2 (**Fig. 4E**).

Intriguingly, the most differentially expressed gene was for the Fas ligand (*Faslg*) and may represent a consistent mechanism of immune escape within the cohort of progressor dogs (cluster 2) with greater *B2m* expression. It has been established that peripheral expression of Fas ligand on multiple cell types in response to inflammatory stimulus promotes deletion of auto-reactive T lymphocytes (e.g., peripheral tolerance; ref. 93), so we examined whether there were compositional differences in the immune compartments from the tumors of the progressor dog cohorts. Using CIBERSORTx (60), the relative abundance of immune cell populations from the bulk NanoString profiling data was estimated. Tumors with reduced *B2m* expression were accompanied by greater populations of canonical tumor-suppressive immune cells (i.e., "M2" polarized macrophages and neutrophils), whereas dogs with higher MHC-I antigen presentation had more activated macrophages and CD4 T lymphocytes (**Fig. 4F**). Together, these differences likely contributed to the poorer prognosis of patients with reduced MHC class I antigen presentation, regardless of the tumor stage at presentation (**Fig. 4G**; log-rank hazard ratio: 4.472).

To explore why the cohort of dogs with higher class I antigen presentation and reduced abundance of immunosuppressive immune populations (cluster 2) still progressed after therapy, gene expression was examined within tissue collected from metastatic tumor sites. Using a gene set describing common genetic mutations that enable immune escape in primary or metastatic tumor tissues (80), the differences in expression between cohorts is diminished in metastatic tumors (**Fig. 4H**). This suggests that metastatic tumors from dogs with higher MHC-I expression at their primary tumors may have been preferentially seeded by tumor subpopulations with greater genetic immune escape, such as MHC-I loss of heterozygosity.

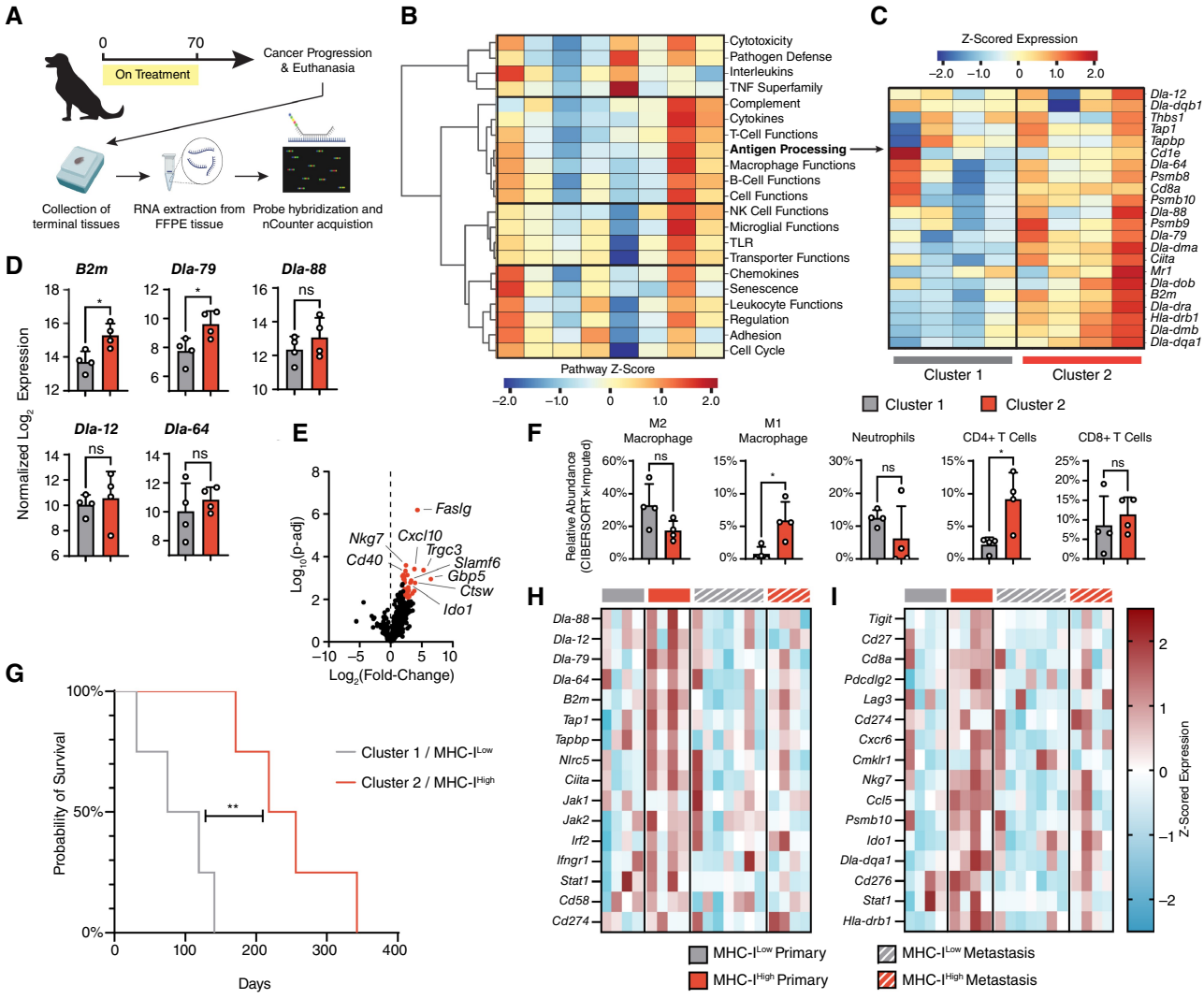

Figure 4.

NanoString RNA profiling of terminal primary and metastatic tumor tissues. **A,** Terminal primary and metastatic tumor tissues from euthanized patients were collected and FFPE processed. RNA was extracted from FFPE tissues and prepared for NanoString analysis with the NanoString nCounter Canine IO panel. **B,** Pathway scoring and hierarchical clustering of NanoString annotated pathways involved in canine cancer immune response. Pathway scores were calculated as the first principal component of the pathway genes normalized expression. Heatmap columns represent individual patients' primary oral melanoma. **C,** *Z*-scored expression of genes related to canine antigen presentation, with grouping of tumor samples into two hierarchical clusters. **D,** Normalized expression (log_2) of MHC class I–related genes. **E,** Volcano plot of differential gene expression of cluster 2 (MHC-I^{Hi}) relative to cluster 1 (MHC-I^{Low}). Genes associated with significant *P*-adjusted values (<0.05) are highlighted in red. **F,** Relative abundance of intratumoral immune populations as determined through application of the CIBERSORTx algorithm on NanoString data. **G,** Survival of MHC-I^{Hi} and MHC-I^{Low} progressor dogs. **H** and **I,** *Z*-scored expression data for genes associated with tumor immune escape (ref. 80; **H**) and response to immune checkpoint blockade (ref. 94; **I**) for patients with primary and metastatic lesions of MHC-I^{Hi} and MHC-I^{Low}. Statistics: Differential gene expression and relative abundance of immune populations compared using one-way ANOVA with Tukey multiple comparisons test. Survival compared with log-rank Mantel–Cox test.*, $P < 0.05$; **, $P < 0.01$. ns, not significant. (**A,** Created with BioRender.com).

We further examined gene expression between cohorts at their primary and metastatic tumors across an annotated set predictive of human response to checkpoint inhibitors (94). We found that only primary tumors of higher expression MHC-I dogs are expected to have a positive response to immunotherapy, consistent with the observed local response, but metastatic progression of these patients follows our combined cytokine treatment (**Fig. 4I**). Overall, these results motivate exploration of treatment combinations to overcome dysfunctional MHC class I antigen presentation in tumors to extend therapeutic benefit to a greater population of pet dogs, with the intention that lessons gleaned from comparative oncology studies can be quickly pivoted to accelerate novel immunotherapeutic strategies to benefit human patients with cancer.

Discussion

Mechanisms of primary and adaptive resistance to immunotherapy contribute to the lack of clinical benefit for a majority of patients with cancer who are treated with antagonistic, checkpoint-

inhibiting antibodies (5). As a result, there have been attempts to combine these therapies with agonistic, or immune-stimulating, agents to overcome tumor resistance mechanisms and drive more durable responses (95, 96). Cytokines, such as IL2 and IL12, are one class of agonistic therapies that have shown great promise against human cancers, but suffer from unacceptable toxicities due to their activation of immune cells throughout the body (15, 16). Approaches to restrict the activity of potent cytokines to tumor have gained momentum, one of which includes the retention of engineered cytokines to tumor extracellular matrix following intratumoral injection (25, 35–37). We and others have previously reported on the safety improvements provided by this strategy of anchoring cytokines to tumor collagen in both mice and pet dogs (25, 35, 51), but the efficacy in advanced canine tumors had been previously unexplored.

In this work, we evaluated the efficacy of tumor-localized IL2 and IL12 cytokines in pet dogs with advanced OMM to potentially predict success of clinically translating this approach. As dogs share key physical features and tumor biology with humans, they have gained traction as models for human comparative oncology (43, 45, 48). Here, we have observed encouraging results for both the antitumor efficacy and tolerability of single-dose RT with repeat intratumoral IL2 and IL12 cytokines. Primary tumor responses were often rapid and durable, with 256-day median survival across all treated cohorts; significantly longer than the historical 65-day median for untreated canine oral melanoma (68). Moreover, many of these responses were observed among dogs in the non-toxic 1× and 2× cohorts, suggesting that the tumor-localization strategy via retention to tumor collagen is clinically promising for safely and effectively treating human malignancies. Locoregional responses at metastatic sites driven by intratumoral therapy achieved an overall biologic response against combined tumor and metastases in 10/13 (76.9%) dogs receiving full therapy, with partial responses in 8/13 (61.5%) dogs (Supplementary Fig. S9). This result provides early evidence that intratumoral treatment with collagen-bound cytokines may potentiate systemic antitumor immunity in pet dogs with naturally occurring cancers. Importantly, these canine tumors develop under evolving tumor immune evasion and suppression mechanisms analogous to those in humans, suggesting that this engineered cytokine approach may achieve similar responses in human clinical trials.

Profiling of dogs that progressed while, or soon after, receiving the RT plus intratumoral cytokine treatment revealed that dysfunctional antigen presentation may contribute to the rapid progression of canine malignant melanoma. This complements a growing list of canine tumor features that overlap with the human hallmarks of cancer, including sustained proliferative signaling (97) and mutations to oncogenic driver or tumor suppressor genes (49, 98). Although less definitive, the dogs with higher MHC class-I expression may have progressed because of tumor microenvironment–induced dysfunction of immune cells. With the observation that *Faslg* and *Ido1* are more highly expressed by these tumors, we suspect that the combination cytokine therapy was actively promoting an antitumor response met by immune counter-regulation, as we have observed previously in canine soft-tissue sarcomas (51). The combination of IL12/IL2 has been described to upregulate the expression of Fas ligand on draining lymph node lymphocytes (99), which, while aiding their ability to kill malignant tumor cells, could contribute to eventual lymphocyte fratricide or suicide (100). This mechanism might contribute to our observation of tachyphylaxis in some of the dogs (**Fig. 2C**). Moreover, the mixed response between primary tumors and metastatic sites may manifest from the varied gene expression landscape and erected barriers to immune function observed between these metastatic tumors and their primary tumor counterparts, suggesting that systemic therapies (such as anti-PD1 antibodies) may be necessary to leverage cytotoxic effector cells primed by local intratumoral therapy (35, 51).

Our learnings from each group of progressing dogs provide actionable insights for future combination treatments to test alongside the intratumoral cytokine approach. To this end, we are interested in evaluating the combination of checkpoint inhibitors with the RT-plus-intratumoral cytokine treatment in future studies, particularly along the PD1/PDL1 axis, because of recent encouraging responses with these immunotherapies observed in local and advanced canine melanoma (101–104). Our prior work with canine soft-tissue sarcomas indicated that checkpoint blockade might relieve counter-regulatory responses to intratumoral cytokine therapy, which we confirmed in the murine B16F10 tumor model (51). However, resistance to intratumoral IL2 and IL12 therapy via beta-2-microglobulin loss and, subsequently, dysfunctional antigen presentation, seem to overlap with known resistance mechanisms to checkpoint inhibitors (91, 105). As a result, future screening of canine *B2m* and MHC class-I–associated gene expression prior to trial enrollment could help accrue patients into separate, more rationally designed, combination treatments. For dogs with reduced or dysfunctional antigen presentation, there have been strategies reported for combining immunotherapies with epigenetic drugs to remove silencing of beta-2-microglobulin and restore MHC-I expression (106–108), in addition to strategies to engage innate immune cells for direct tumor-cell killing (109–111) or to coordinate their licensing of antigen-independent killing by $CD8^+$ lymphocytes (112, 113). Finally, given our observation of tachyphylaxis in response to repeat cytokine dosing and reports of the importance for immune rest in engineered CAR-T therapies (114), we are interested in exploring longer intervals between cytokine doses or separately administering individual cytokines to minimize activation-induced cell death or induced dysfunction of primed $CD8^+$ T cells.

Overall, this work highlights the benefit of preclinical evaluation of a novel immunotherapy alongside current standard of care in a more human-analogous cancer model than mouse tumors. While statistical power of such a trial in pet dogs is more limited, we argue that the value gained in predictive efficacy, safety, and resistance to therapy is obtained at dramatically lesser expense and greater speed than a corresponding human clinical trial. Exploitation of canine trials as a bridge from murine studies to the clinic should be expanded to reap these benefits more widely. Certain methodology to maximize value from these canine cancer trials stands to gain from broader investigation as well. We recognize that a primary limitation of this study is the lack of longitudinal sampling from canine tumors to characterize the evolution of antitumor responses and resistance to cytokine treatment. Through comparative oncologic testing, we anticipate a greater likelihood of future clinical success for our collagen-binding cytokine approach, as well as more broadly for other novel immunotherapies investigated in pet dogs with cancer.

Authors' Disclosures

N. Momin reports personal fees from Cullinan Therapeutics outside the submitted work, as well as a patent for US20200102370A1, licensed to Cullinan Therapeutics. E. Fink reports grants from NIH during the conduct of the study. K.D. Wittrup reports other support from Cullinan Therapeutics outside the submitted work. No disclosures were reported by the other authors.

Authors' Contributions

J.A. Stinson: Conceptualization, formal analysis, investigation, writing–original draft, writing–review and editing. **M.M.P. Barbosa:** Conceptualization, formal analysis, investigation, writing–original draft, writing–review and editing. **A. Sheen:** Conceptualization, formal analysis, investigation, writing–review and editing. **N. Momin:** Conceptualization, formal analysis, investigation, writing–review and editing. **E. Fink:** Formal analysis, investigation, writing–review and editing. **J. Hampel:** Investigation, writing–review and editing. **K.A. Selting:** Formal analysis, investigation, writing–review and editing. **R.L. Kamerer:** Investigation, writing–review and editing. **K.L. Bailey:** Formal analysis, investigation, writing–review and editing. **K.D. Wittrup:** Conceptualization, formal analysis, funding acquisition, investigation, writing–original draft, writing–review and editing. **T.M. Fan:** Conceptualization, formal analysis, funding acquisition, investigation, writing–original draft, writing–review and editing.

Acknowledgments

We gratefully thank all of our pet dog owners for their consent and willingness to participate in this investigational trial. This study was supported by National Cancer Institute grant R01CA271243 (T.M. Fan and K.D. Wittrup), NIBIB grant R01EB031082 (K.D. Wittrup), and GRFP (A. Sheen). The authors would like to acknowledge Dr. Amy Schnelle and the Tumor Engineering and Phenotyping Shared Resource at the Cancer Center at Illinois for assistance with histology and immunohistochemistry analysis.

Note

Supplementary data for this article are available at Clinical Cancer Research Online (http://clincancerres.aacrjournals.org/).

Received March 15, 2024; revised May 8, 2024; accepted July 3, 2024; published first July 9, 2024.

References

1. Larkin J, Chiarion-Sileni V, Gonzalez R, Grob J-J, Rutkowski P, Lao CD, et al. Five-year survival with combined nivolumab and ipilimumab in advanced melanoma. N Engl J Med 2019;381:1535–46.
2. Topalian SL, Hodi FS, Brahmer JR, Gettinger SN, Smith DC, McDermott DF, et al. Five-year survival and correlates among patients with advanced melanoma, renal cell carcinoma, or non-small cell lung cancer treated with nivolumab. JAMA Oncol 2019;5:1411–20.
3. Robert C, Carlino MS, McNeil C, Ribas A, Grob J-J, Schachter J, et al. Seven-year follow-up of the phase III KEYNOTE-006 study: pembrolizumab versus ipilimumab in advanced melanoma. J Clin Oncol 2023;41:3998–4003.
4. Cogdill AP, Andrews MC, Wargo JA. Hallmarks of response to immune checkpoint blockade. Br J Cancer 2017;117:1–7.
5. Sharma P, Hu-Lieskovan S, Wargo JA, Ribas A. Primary, adaptive, and acquired resistance to cancer immunotherapy. Cell 2017;168:707–23.
6. Koyama S, Akbay EA, Li YY, Herter-Sprie GS, Buczkowski KA, Richards WG, et al. Adaptive resistance to therapeutic PD-1 blockade is associated with upregulation of alternative immune checkpoints. Nat Commun 2016;7:10501.
7. Yuan J, Khilnani A, Brody J, Andtbacka RHI, Hu-Lieskovan S, Luke JJ, et al. Current strategies for intratumoural immunotherapy–beyond immune checkpoint inhibition. Eur J Cancer 2021;157:493–510.
8. Weber R, Fleming V, Hu X, Nagibin V, Groth C, Altevogt P, et al. Myeloid-derived suppressor cells hinder the anti-cancer activity of immune checkpoint inhibitors. Front Immunol 2018;9:1310.
9. Briukhovetska D, Dörr J, Endres S, Libby P, Dinarello CA, Kobold S. Interleukins in cancer: from biology to therapy. Nat Rev Cancer 2021;21:481–99.
10. Wigginton JM, Wiltrout RH. IL-12/IL-2 combination cytokine therapy for solid tumours: translation from bench to bedside. Expert Opin Biol Ther 2002;2:513–24.
11. Buchbinder EI, Dutcher JP, Daniels GA, Curti BD, Patel SP, Holtan SG, et al. Therapy with high-dose Interleukin-2 (HD IL-2) in metastatic melanoma and renal cell carcinoma following PD1 or PDL1 inhibition. J Immunother Cancer 2019;7:49.
12. Falchook G, Gan H, Fu S, McKean M, Azad A, Sommerhalder D, et al. Phase 1/2 study of THOR-707 (SAR444245), a pegylated recombinant non-alpha IL-2, as monotherapy and in combination with pembrolizumab or cetuximab in patients (pts) with advanced solid tumors. J Immunother Cancer 2021;9:A511.
13. Algazi AP, Twitty CG, Tsai KK, Le M, Pierce R, Browning E, et al. Phase II trial of IL-12 plasmid transfection and PD-1 blockade in immunologically quiescent melanoma. Clin Cancer Res 2020;26:2827–37.
14. Lotze MT, Matory YL, Ettinghausen SE, Rayner AA, Sharrow SO, Seipp CA, et al. *In vivo* administration of purified human interleukin 2. II. Half life, immunologic effects, and expansion of peripheral lymphoid cells *in vivo* with recombinant IL 2. J Immunol 1985;135:2865–75.
15. Berraondo P, Sanmamed MF, Ochoa MC, Etxeberria I, Aznar MA, Pérez-Gracia JL, et al. Cytokines in clinical cancer immunotherapy. Br J Cancer 2019;120:6–15.
16. Santollani L, Wittrup KD. Spatiotemporally programming cytokine immunotherapies through protein engineering. Immunol Rev 2023;320:10–28.
17. Hutmacher C, Neri D. Antibody-cytokine fusion proteins: biopharmaceuticals with immunomodulatory properties for cancer therapy. Adv Drug Deliv Rev 2019;141:67–91.
18. Garcin G, Paul F, Staufenbiel M, Bordat Y, Van der Heyden J, Wilmes S, et al. High efficiency cell-specific targeting of cytokine activity. Nat Commun 2014;5:3016.
19. Gillies SD, Lan Y, Wesolowski JS, Qian X, Reisfeld RA, Holden S, et al. Antibody-IL-12 fusion proteins are effective in SCID mouse models of prostate and colon carcinoma metastases. J Immunol 1998;160:6195–203.
20. Fallon J, Tighe R, Kradjian G, Guzman W, Bernhardt A, Neuteboom B, et al. The immunocytokine NHS-IL12 as a potential cancer therapeutic. Oncotarget 2014;5:1869–84.
21. Wieckowski S, Hemmerle T, Prince SS, Schlienger BD, Hillinger S, Neri D, et al. Therapeutic efficacy of the F8-IL2 immunocytokine in a metastatic mouse model of lung adenocarcinoma. Lung Cancer 2015;88:9–15.
22. Venetz D, Koovely D, Weder B, Neri D. Targeted reconstitution of cytokine activity upon antigen binding using split cytokine antibody fusion proteins. J Biol Chem 2016;291:18139–47.
23. Steiner P, Brodkin H, Canales J, Hicklin D, Isaacs R, Ismail N, et al. Conditionally activated IL-12 or IFNα Indukine molecules inhibit syngeneic lymphoma tumor growth in mice, induce anti-tumor immune responses and are tolerated in non-human primates. Blood 2021;138(Suppl 1):2258.
24. Nirschl CJ, Brodkin HR, Hicklin DJ, Ismail N, Morris K, Seidel-Dugan C, et al. Discovery of a conditionally activated IL-2 that promotes antitumor immunity and induces tumor regression. Cancer Immunol Res 2022;10:581–96.
25. Mansurov A, Ishihara J, Hosseinchi P, Potin L, Marchell TM, Ishihara A, et al. Collagen-binding IL-12 enhances tumour inflammation and drives the complete remission of established immunologically cold mouse tumours. Nat Biomed Eng 2020;4:531–43.
26. Xue D, Moon B, Liao J, Guo J, Zou Z, Han Y, et al. A tumor-specific pro-IL-12 activates preexisting cytotoxic T cells to control established tumors. Sci Immunol 2022;7:eabi6899.
27. Levin AM, Bates DL, Ring AM, Krieg C, Lin JT, Su L, et al. Exploiting a natural conformational switch to engineer an interleukin-2 "superkine". Nature 2012;484:529–33.
28. Sun Z, Ren Z, Yang K, Liu Z, Cao S, Deng S, et al. A next-generation tumor-targeting IL-2 preferentially promotes tumor-infiltrating $CD8^+$ T-cell response and effective tumor control. Nat Commun 2019;10:3874.
29. Charych DH, Hoch U, Langowski JL, Lee SR, Addepalli MK, Kirk PB, et al. NKTR-214, an engineered cytokine with biased IL2 receptor binding, increased tumor exposure, and marked efficacy in mouse tumor models. Clin Cancer Res 2016;22:680–90.
30. Chen X, Ai X, Wu C, Wang H, Zeng G, Yang P, et al. A novel human IL-2 mutein with minimal systemic toxicity exerts greater antitumor efficacy than wild-type IL-2. Cell Death Dis 2018;9:989.
31. Agarwal Y, Milling LE, Chang JYH, Santollani L, Sheen A, Lutz EA, et al. Intratumourally injected alum-tethered cytokines elicit potent and safer local and systemic anticancer immunity. Nat Biomed Eng 2022;6:129–43.
32. Lutz EA, Agarwal Y, Momin N, Cowles SC, Palmeri JR, Duong E, et al. Alum-anchored intratumoral retention improves the tolerability and antitumor efficacy of type I interferon therapies. Proc Natl Acad Sci U S A 2022;119:e2205983119.
33. Zaharoff DA, Hance KW, Rogers CJ, Schlom J, Greiner JW. Intratumoral immunotherapy of established solid tumors with chitosan/IL-12. J Immunother 2010;33:697–705.

34. Park CG, Hartl CA, Schmid D, Carmona EM, Kim H-J, Goldberg MS. Extended release of perioperative immunotherapy prevents tumor recurrence and eliminates metastases. Sci Transl Med 2018;10:eaar1916.
35. Momin N, Mehta NK, Bennett NR, Ma L, Palmeri JR, Chinn MM, et al. Anchoring of intratumorally administered cytokines to collagen safely potentiates systemic cancer immunotherapy. Sci Transl Med 2019;11:eaaw2614.
36. Ishihara J, Ishihara A, Sasaki K, Lee SS-Y, Williford J-M, Yasui M, et al. Targeted antibody and cytokine cancer immunotherapies through collagen affinity. Sci Transl Med 2019;11:eaau3259.
37. Momin N, Palmeri JR, Lutz EA, Jailkhani N, Mak H, Tabet A, et al. Maximizing response to intratumoral immunotherapy in mice by tuning local retention. Nat Commun 2022;13:109.
38. Zitvogel L, Pitt JM, Daillère R, Smyth MJ, Kroemer G. Mouse models in oncoimmunology. Nat Rev Cancer 2016;16:759–73.
39. Buqué A, Galluzzi L. Modeling tumor immunology and immunotherapy in mice. Trends Cancer 2018;4:599–601.
40. Mak IW, Evaniew N, Ghert M. Lost in translation: animal models and clinical trials in cancer treatment. Am J Transl Res 2014;6:114–8.
41. Wong CH, Siah KW, Lo AW. Estimation of clinical trial success rates and related parameters. Biostatistics 2019;20:273–86.
42. Ireson CR, Alavijeh MS, Palmer AM, Fowler ER, Jones HJ. The role of mouse tumour models in the discovery and development of anticancer drugs. Br J Cancer 2019;121:101–8.
43. Rowell JL, McCarthy DO, Alvarez CE. Dog models of naturally occurring cancer. Trends Mol Med 2011;17:380–8.
44. Gardner HL, Fenger JM, London CA. Dogs as a model for cancer. Annu Rev Anim Biosci 2016;4:199–222.
45. Von Rueden SK, Fan TM. Cancer-immunity cycle and therapeutic interventions- opportunities for including pet dogs with cancer. Front Oncol 2021;11:773420.
46. Schiffman JD, Breen M. Comparative oncology: what dogs and other species can teach us about humans with cancer. Philos Trans R Soc Lond B Biol Sci 2015;370:20140231.
47. Park JS, Withers SS, Modiano JF, Kent MS, Chen M, Luna JI, et al. Canine cancer immunotherapy studies: linking mouse and human. J Immunother Cancer 2016;4:97.
48. LeBlanc AK, Mazcko CN. Improving human cancer therapy through the evaluation of pet dogs. Nat Rev Cancer 2020;20:727–42.
49. Wu K, Rodrigues L, Post G, Harvey G, White M, Miller A, et al. Analyses of canine cancer mutations and treatment outcomes using real-world clinico-genomics data of 2119 dogs. NPJ Precis Oncol 2023;7:8.
50. Alsaihati BA, Ho K-L, Watson J, Feng Y, Wang T, Dobbin KK, et al. Canine tumor mutational burden is correlated with TP53 mutation across tumor types and breeds. Nat Commun 2021;12:4670.
51. Stinson JA, Sheen A, Momin N, Hampel J, Bernstein R, Kamerer R, et al. Collagen-anchored interleukin-2 and interleukin-12 safely reprogram the tumor microenvironment in canine soft-tissue sarcomas. Clin Cancer Res 2023;29:2110–22.
52. Smith SH, Goldschmidt MH, McManus PM. A comparative review of melanocytic neoplasms. Vet Pathol 2002;39:651–78.
53. Bergman PJ. Canine oral melanoma. Clin Tech Small Anim Pract 2007;22:55–60.
54. Eton O, Rosenblum MG, Legha SS, Zhang W, Jo East M, Bedikian A, et al. Phase I trial of subcutaneous recombinant human interleukin-2 in patients with metastatic melanoma. Cancer 2002;95:127–34.
55. Dutcher JP, Schwartzentruber DJ, Kaufman HL, Agarwala SS, Tarhini AA, Lowder JN, et al. High dose interleukin-2 (Aldesleukin)—expert consensus on best management practices-2014. J Immunother Cancer 2014;2:26.
56. Pachella LA, Madsen LT, Dains JE. The toxicity and benefit of various dosing strategies for interleukin-2 in metastatic melanoma and renal cell carcinoma. J Adv Pract Oncol 2015;6:212–21.
57. Paoloni M, Mazcko C, Selting K, Lana S, Barber L, Phillips J, et al. Defining the pharmacodynamic profile and therapeutic index of NHS-IL12 immunocytokine in dogs with malignant melanoma. PLoS One 2015;10:e0129954.
58. LeBlanc AK, Atherton M, Bentley RT, Boudreau CE, Burton JH, Curran KM, et al. Veterinary Cooperative Oncology Group-Common Terminology Criteria for Adverse Events (VCOG-CTCAE v2) following investigational therapy in dogs and cats. Vet Comp Oncol 2021;19:311–52.
59. Nguyen SM, Thamm DH, Vail DM, London CA. Response evaluation criteria for solid tumours in dogs (v1.0): a Veterinary Cooperative Oncology Group (VCOG) consensus document. Vet Comp Oncol 2015;13:176–83.
60. Newman AM, Steen CB, Liu CL, Gentles AJ, Chaudhuri AA, Scherer F, et al. Determining cell type abundance and expression from bulk tissues with digital cytometry. Nat Biotechnol 2019;37:773–82.
61. Sobottka B, Nowak M, Frei AL, Haberecker M, Merki S, et al; Tumor Profiler consortium. Establishing standardized immune phenotyping of metastatic melanoma by digital pathology. Lab Invest 2021;101:1561–70.
62. Bateman KE, Catton PA, Pennock PW, Kruth SA. 0-7-21 radiation therapy for the treatment of canine oral melanoma. J Vet Intern Med 1994;8:267–72.
63. Blackwood L, Dobson JM. Radiotherapy of oral malignant melanomas in dogs. J Am Vet Med Assoc 1996;209:98–102.
64. Proulx DR, Ruslander DM, Dodge RK, Hauck ML, Williams LE, Horn B, et al. A retrospective analysis of 140 dogs with oral melanoma treated with external beam radiation. Vet Radiol Ultrasound 2003;44:352–9.
65. Marciscano AE, Ghasemzadeh A, Nirschl TR, Theodros D, Kochel CM, Francica BJ, et al. Elective nodal irradiation attenuates the combinatorial efficacy of stereotactic radiation therapy and immunotherapy. Clin Cancer Res 2018;24:5058–71.
66. Cho Y, Park S, Byun HK, Lee CG, Cho J, Hong MH, et al. Impact of treatment-related lymphopenia on immunotherapy for advanced non-small cell lung cancer. Int J Radiat Oncol Biol Phys 2019;105:1065–73.
67. Saddawi-Konefka R, O'Farrell A, Faraji F, Clubb L, Allevato MM, Jensen SM, et al. Lymphatic-preserving treatment sequencing with immune checkpoint inhibition unleashes cDC1-dependent antitumor immunity in HNSCC. Nat Commun 2022;13:4298.
68. Pazzi P, Steenkamp G, Rixon AJ. Treatment of canine oral melanomas: a critical review of the literature. Vet Sci 2022;9:196.
69. Donnelly RP, Young HA, Rosenberg AS. An overview of cytokines and cytokine antagonists as therapeutic agents. Ann N Y Acad Sci 2009;1182:1–13.
70. Saxton RA, Glassman CR, Garcia KC. Emerging principles of cytokine pharmacology and therapeutics. Nat Rev Drug Discov 2023;22:21–37.
71. Cope A, Le Friec G, Cardone J, Kemper C. The Th1 life cycle: molecular control of IFN-γ to IL-10 switching. Trends Immunol 2011;32:278–86.
72. Gillies SD, Lan Y, Brunkhorst B, Wong W-K, Li Y, Lo K-M. Bi-functional cytokine fusion proteins for gene therapy and antibody-targeted treatment of cancer. Cancer Immunol Immunother 2002;51:449–60.
73. Schwarz E, Carson WE III. Analysis of potential biomarkers of response to IL-12 therapy. J Leukoc Biol 2022;112:557–67.
74. Dighe AS, Richards E, Old LJ, Schreiber RD. Enhanced in vivo growth and resistance to rejection of tumor cells expressing dominant negative IFN gamma receptors. Immun 1994;1:447–56.
75. Castro F, Cardoso AP, Gonçalves RM, Serre K, Oliveira MJ. Interferon-gamma at the crossroads of tumor immune surveillance or evasion. Front Immunol 2018;9:847.
76. Bromberg JF, Horvath CM, Wen Z, Schreiber RD, Darnell JE Jr. Transcriptionally active Stat1 is required for the antiproliferative effects of both interferon alpha and interferon gamma. Proc Natl Acad Sci U S A 1996;93:7673–8.
77. Kaplan DH, Shankaran V, Dighe AS, Stockert E, Aguet M, Old LJ, et al. Demonstration of an interferon gamma-dependent tumor surveillance system in immunocompetent mice. Proc Natl Acad Sci U S A 1998;95:7556–61.
78. Martínez-Jiménez F, Movasati A, Brunner SR, Nguyen L, Priestley P, Cuppen E, et al. Pan-cancer whole-genome comparison of primary and metastatic solid tumours. Nature 2023;618:333–41.
79. Yates LR, Knappskog S, Wedge D, Farmery JHR, Gonzalez S, Martincorena I, et al. Genomic evolution of breast cancer metastasis and relapse. Cancer Cell 2017;32:169–84.e7.
80. Martínez-Jiménez F, Priestley P, Shale C, Baber J, Rozemuller E, Cuppen E. Genetic immune escape landscape in primary and metastatic cancer. Nat Genet 2023;55:820–31.
81. Wei J, Montalvo-Ortiz W, Yu L, Krasco A, Ebstein S, Cortez C, et al. Sequence of αPD-1 relative to local tumor irradiation determines the induction of abscopal antitumor immune responses. Sci Immunol 2021;6:eabg0117.
82. Demaria S, Kawashima N, Yang AM, Devitt ML, Babb JS, Allison JP, et al. Immune-mediated inhibition of metastases after treatment with local radiation and CTLA-4 blockade in a mouse model of breast cancer. Clin Cancer Res 2005;11:728–34.
83. Formenti SC, Rudqvist N-P, Golden E, Cooper B, Wennerberg E, Lhuillier C, et al. Radiotherapy induces responses of lung cancer to CTLA-4 blockade. Nat Med 2018;24:1845–51.
84. Seung SK, Curti BD, Crittenden M, Walker E, Coffey T, Siebert JC, et al. Phase 1 study of stereotactic body radiotherapy and interleukin-2-tumor and immunological responses. Sci Transl Med 2012;4:137ra74.

85. Mills BN, Connolly KA, Ye J, Murphy JD, Uccello TP, Han BJ, et al. Stereotactic body radiation and interleukin-12 combination therapy eradicates pancreatic tumors by repolarizing the immune microenvironment. Cell Rep 2019;29:406–21.e5.
86. Andtbacka RHI, Kaufman HL, Collichio F, Amatruda T, Senzer N, Chesney J, et al. Talimogene laherparepvec improves durable response rate in patients with advanced melanoma. J Clin Oncol 2015;33:2780–8.
87. Challis GB, Stam HJ. The spontaneous regression of cancer. A review of cases from 1900 to 1987. Acta Oncol 1990;29:545–50.
88. Sousa de LG, McGrail DJ, Li K, Marques-Piubelli ML, Gonzalez C, Dai H, et al. Spontaneous tumor regression following COVID-19 vaccination. J Immunother Cancer 2022;10:e004371.
89. Quezada SA, Peggs KS, Curran MA, Allison JP. CTLA4 blockade and GM-CSF combination immunotherapy alters the intratumor balance of effector and regulatory T cells. J Clin Invest 2006;116:1935–45.
90. Liakou CI, Kamat A, Tang DN, Chen H, Sun J, Troncoso P, et al. CTLA-4 blockade increases IFNgamma-producing CD4$^+$ICOShi cells to shift the ratio of effector to regulatory T cells in cancer patients. Proc Natl Acad Sci U S A 2008;105:14987–92.
91. Sade-Feldman M, Jiao YJ, Chen JH, Rooney MS, Barzily-Rokni M, Eliane J-P, et al. Resistance to checkpoint blockade therapy through inactivation of antigen presentation. Nat Commun 2017;8:1136.
92. Beatty GL, Gladney WL. Immune escape mechanisms as a guide for cancer immunotherapy. Clin Cancer Res 2015;21:687–92.
93. Bonfoco E, Stuart PM, Brunner T, Lin T, Griffith TS, Gao Y, et al. Inducible nonlymphoid expression of Fas ligand is responsible for superantigen-induced peripheral deletion of T cells. Immunity 1998;9:711–20.
94. Ayers M, Lunceford J, Nebozhyn M, Murphy E, Loboda A, Kaufman DR, et al. IFN-γ-related mRNA profile predicts clinical response to PD-1 blockade. J Clin Invest 2017;127:2930–40.
95. Anderson KG, Stromnes IM, Greenberg PD. Obstacles posed by the tumor microenvironment to T cell activity: a case for synergistic therapies. Cancer Cell 2017;31:311–25.
96. Veillette A, Davidson D. Developing combination immunotherapies against cancer that make sense. Sci Immunol 2018;3:eaav1872.
97. Fowles JS, Denton CL, Gustafson DL. Comparative analysis of MAPK and PI3K/AKT pathway activation and inhibition in human and canine melanoma. Vet Comp Oncol 2015;13:288–304.
98. Kim T-M, Yang IS, Seung B-J, Lee S, Kim D, Ha Y-J, et al. Cross-species oncogenic signatures of breast cancer in canine mammary tumors. Nat Commun 2020;11:3616.
99. Wigginton JM, Gruys E, Geiselhart L, Subleski J, Komschlies KL, Park JW, et al. IFN-gamma and Fas/FasL are required for the antitumor and antiangiogenic effects of IL-12/pulse IL-2 therapy. J Clin Invest 2001;108:51–62.
100. Li J-H, Rosen D, Sondel P, Berke G. Immune privilege and FasL: two ways to inactivate effector cytotoxic T lymphocytes by FasL-expressing cells. Immunology 2002;105:267–77.
101. Maekawa N, Konnai S, Takagi S, Kagawa Y, Okagawa T, Nishimori A, et al. A canine chimeric monoclonal antibody targeting PD-L1 and its clinical efficacy in canine oral malignant melanoma or undifferentiated sarcoma. Sci Rep 2017;7:8951.
102. Maekawa N, Konnai S, Nishimura M, Kagawa Y, Takagi S, Hosoya K, et al. PD-L1 immunohistochemistry for canine cancers and clinical benefit of anti-PD-L1 antibody in dogs with pulmonary metastatic oral malignant melanoma. NPJ Precis Oncol 2021;5:10.
103. Igase M, Nemoto Y, Itamoto K, Tani K, Nakaichi M, Sakurai M, et al. A pilot clinical study of the therapeutic antibody against canine PD-1 for advanced spontaneous cancers in dogs. Sci Rep 2020;10:18311.
104. Igase M, Inanaga S, Tani K, Nakaichi M, Sakai Y, Sakurai M, et al. Long-term survival of dogs with stage 4 oral malignant melanoma treated with anti-canine PD-1 therapeutic antibody: a follow-up case report. Vet Comp Oncol 2022;20:901–5.
105. Zaretsky JM, Garcia-Diaz A, Shin DS, Escuin-Ordinas H, Hugo W, Hu-Lieskovan S, et al. Mutations associated with acquired resistance to PD-1 blockade in melanoma. N Engl J Med 2016;375:819–29.
106. Hicks KC, Chariou PL, Ozawa Y, Minnar CM, Knudson KM, Meyer TJ, et al. Tumour-targeted interleukin-12 and entinostat combination therapy improves cancer survival by reprogramming the tumour immune cell landscape. Nat Commun 2021;12:5151.
107. Hogg SJ, Beavis PA, Dawson MA, Johnstone RW. Targeting the epigenetic regulation of antitumour immunity. Nat Rev Drug Discov 2020;19:776–800.
108. Liu Z, Ren Y, Weng S, Xu H, Li L, Han X. A new trend in cancer treatment: the combination of epigenetics and immunotherapy. Front Immunol 2022;13:809761.
109. Wang C, Cui A, Bukenya M, Aung A, Pradhan D, Whittaker CA, et al. Reprogramming NK cells and macrophages via combined antibody and cytokine therapy primes tumors for elimination by checkpoint blockade. Cell Rep 2021;37:110021.
110. Hirschhorn D, Budhu S, Kraehenbuehl L, Gigoux M, Schröder D, Chow A, et al. T cell immunotherapies engage neutrophils to eliminate tumor antigen escape variants. Cell 2023;186:1432–47.e17.
111. Linde IL, Prestwood TR, Qiu J, Pilarowski G, Linde MH, Zhang X, et al. Neutrophil-activating therapy for the treatment of cancer. Cancer Cell 2023;41:356–72.e10.
112. Lerner EC, Woroniecka KI, D'Anniballe VM, Wilkinson DS, Mohan AA, Lorrey SJ, et al. CD8$^+$ T cells maintain killing of MHC-I-negative tumor cells through the NKG2D-NKG2DL axis. Nat Cancer 2023;4:1258–72.
113. Kruse B, Buzzai AC, Shridhar N, Braun AD, Gellert S, Knauth K, et al. CD4$^+$ T cell-induced inflammatory cell death controls immune-evasive tumours. Nature 2023;618:1033–40.
114. Weber EW, Parker KR, Sotillo E, Lynn RC, Anbunathan H, Lattin J, et al. Transient rest restores functionality in exhausted CAR-T cells through epigenetic remodeling. Science 2021;372:eaba1786.